Neuron
Article

# Hearing Illusory Sounds in Noise: The Timing of Sensory-Perceptual Transformations in Auditory Cortex

Lars Riecke,[1,*] Fabrizio Esposito,[1,2] Milene Bonte,[1] and Elia Formisano[1]
[1]Department of Cognitive Neuroscience, Faculty of Psychology and Neuroscience, Maastricht University, 6200 MD Maastricht, The Netherlands
[2]Department of Neuroscience, University of Naples "Federico II," 80131 Naples, Italy
*Correspondence: l.riecke@maastrichtuniversity.nl
DOI 10.1016/j.neuron.2009.10.016

## SUMMARY

**Constructive mechanisms in the auditory system may restore a fragmented sound when a gap in this sound is rendered inaudible by noise to yield a continuity illusion. Using combined psychoacoustic and electroencephalography experiments in humans, we found that the sensory-perceptual mechanisms that enable restoration suppress auditory cortical encoding of gaps in interrupted sounds. When physically interrupted tones are perceptually restored, stimulus-evoked synchronization of cortical oscillations at ~4 Hz is suppressed as if physically uninterrupted sounds were encoded. The restoration-specific suppression is induced most strongly in primary-like regions in the right auditory cortex during illusorily filled gaps and also shortly before and after these gaps. Our results reveal that spontaneous modulations in slow evoked auditory cortical oscillations that are involved in encoding acoustic boundaries may determine the perceived continuity of sounds in noise. Such fluctuations could facilitate stable hearing of fragmented sounds in natural environments.**

## INTRODUCTION

In natural scenes, the tracking of relevant sounds is typically complicated by the concurrence of other irrelevant sounds. Nevertheless, the auditory system is remarkably reliable in restoring sounds of interest even when they are partially masked. This constructive nature of hearing is illustrated by the auditory continuity illusion (Miller and Licklider, 1950), in which a physically interrupted sound is heard as continuing through noise. Auditory restoration may arise when a noise burst masks gaps in a sound so that the fragmented sound can be bound with the noise and perceived as holistically continuous (Houtgast, 1972; Warren et al., 1972). Such restoration phenomena have been observed for several sound types, such as tones, sweeps, melodies, voices, and speech (for reviews see Bregman, 1990; Warren, 1999), and in several species, including birds, cats, monkeys, and humans (Sugita, 1997; Braaten and Leary, 1999; Miller et al., 2001; Petkov et al., 2003), suggesting general auditory mechanisms that compensate for the masking and stabilize the hearing of interrupted sounds in noisy environments.

Several neurophysiologic studies found that the masking of acoustic gaps correlates with activity in the auditory cortex (AC) and argued for a role of this brain region in auditory restoration (Sugita, 1997; Micheyl et al., 2003; Petkov et al., 2007; Heinrich et al., 2008; see also Schreiner, 1980). However, none of these studies obtained subjective reports of restoration during the physiologic measurements and incorporated them in the analysis. A more direct link between perception and physiology could be established by investigations of restorations reported during functional magnetic resonance imaging (fMRI), which showed that listeners' subjective experience of restoration is paralleled by hemodynamic activities in primary regions of the right AC (Riecke et al., 2007; Shahin et al., 2009). These results suggested a role of early sensory processes in restoration, but the low temporal resolution of fMRI prevented these studies from further clarifying *how* and *when* perceptually restored sounds may arise from fragmented sensory input.

According to the classical psychoacoustic view, restoration may involve schema-based mechanisms that operate *after* interruptions (Ciocca and Bregman, 1987; Bregman, 1990). However, more recent electrophysiology findings on nonillusory phenomena (for reviews see Engel and Singer, 2001; Schroeder and Lakatos, 2008, 2009) show that sensory-perceptual mechanisms can operate early during stimulus analysis. Specifically, slow neuronal oscillations in the delta and theta range can control the encoding of sensory input (Lakatos et al., 2005, 2007, 2008) especially in the right AC (Luo and Poeppel, 2007). These neuronal oscillations could thus also constitute a relevant mechanism for restoration given the suggested role of early sensory processes in right AC for restoration (Petkov et al., 2007; Riecke et al., 2007; Shahin et al., 2009).

In the present study, we investigated the timing of sensory-perceptual processes associated with the encoding of physically interrupted sounds and their auditory restoration, respectively, by combining behavioral measures with oscillatory electroencephalography (EEG) measures. Listeners were presented with schematic auditory scenes assembled of an interrupted or uninterrupted tone (target) and noise (Figure 1A). The masking of the 600 ms gap was parameterized, including ambiguous conditions

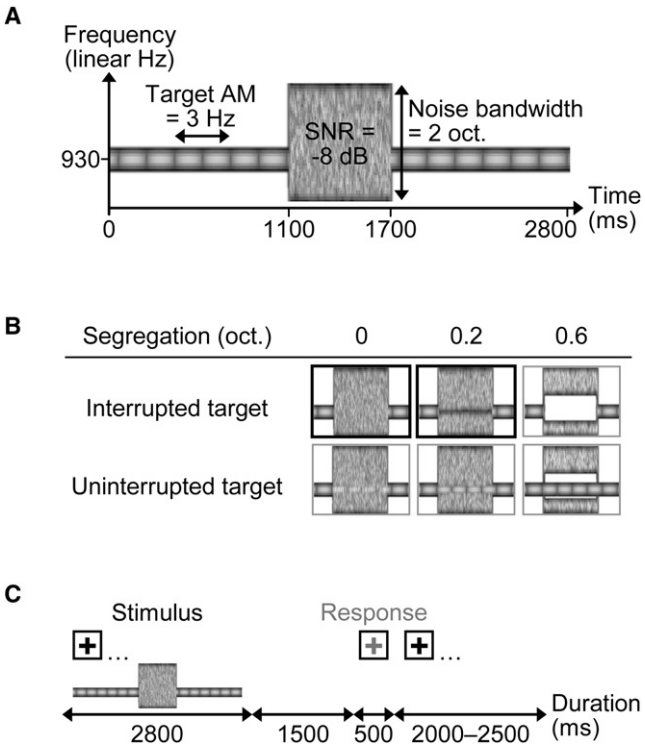


**Figure 1. Schematic Auditory Scene Stimuli and Continuity Rating Task**

(A) Stimuli comprised a tone (target) and interrupting noise.

(B) The target was physically interrupted or uninterrupted, and its masking was parameterized by varying its segregation from the noise with a spectral gap. Two ambiguous conditions, including an individually defined threshold (truncated spectrograms outlined in black), were designed to evoke bistable percepts (i.e., switches in restoration).

(C) Listeners attended to targets and rated their continuity on a four-point scale after a delay during EEG measurements. Stimulus and response intervals were indexed by visual cues and interleaved with silent intervals. AM, amplitude modulation; SNR, signal-to-noise ratio; oct., octaves.

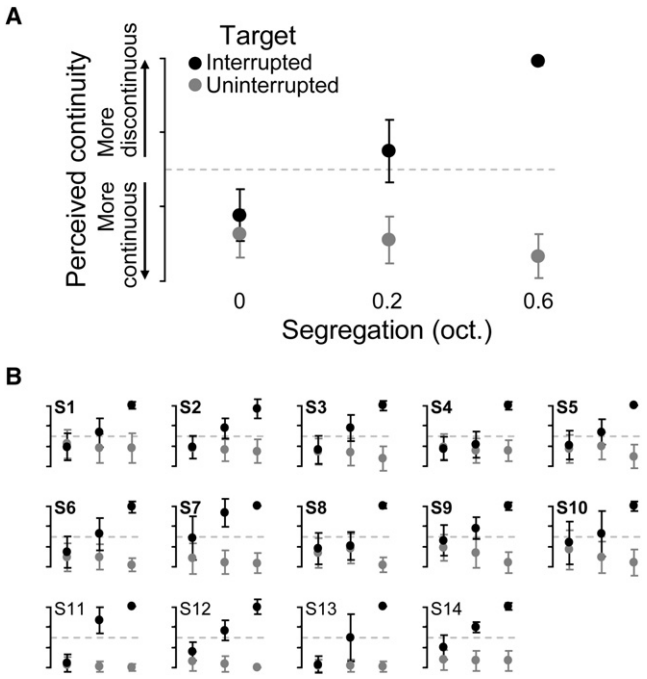


**Figure 2. Masking Effects and Switches in Restoration**

Continuity rating of each stimulus averaged across listeners (A) and across trials for all listeners (B). Unmasking (induced by segregating the noise from the target band) facilitated the detection of the gap in interrupted targets. The ambiguous conditions evoked frequent switches in the restoration of the interrupted target in ten listeners (B, bold indices), as indicated by the standard deviation bars overlapping with the midpoint of the rating scale (dashed line). oct., octaves.

specifically designed to evoke bistable percepts (Figure 1B). Auditory restoration was assessed based on listeners' ratings of the target's continuity (Figure 1C), while scalp potentials were recorded simultaneously. Stimuli and task were fine-tuned previously (Riecke et al., 2008) and identical to those used in our fMRI investigation (Riecke et al., 2007). We hypothesized that restorations of interrupted sounds would be reflected in slow oscillatory activity in the right AC early during stimulus encoding.

## RESULTS

### Behavioral Results

Decreases in masking disrupted continuity illusions of the interrupted target (masking effect, $F_{2,26} = 165.6$, $p < 10^{-15}$; Figure 2A, black circles) and revealed the true continuity of the uninterrupted target (masking effect, $F_{2,26} = 16.4$, $p < 10^{-5}$; gray circles; masking × gap interaction, $F_{2,12} = 383.9$, $p < 10^{-11}$) as observed previously (Riecke et al., 2007, 2008). The ambiguous conditions evoked bistable percepts of the interrupted target as expected: ratings of the same stimulus switched frequently between illusory continuity and true discontinuity (Figure 2B), enabling analysis of stimulus-independent switches in restoration (see Experimental Procedures).

### Stimulus Effects on EEG Oscillations

Scalp EEG data were decomposed into maximally temporally independent components (ICs) and to enable group analyses, individual ICs were clustered based on topographical-functional similarities (see Experimental Procedures). An IC cluster whose features were most indicative of auditory cortical processes showed robust power changes in slow EEG oscillations (Figure 3).

Further analysis of this cluster revealed that theta (3–7 Hz) power increased largely in the noise interval relative to baseline in all stimulus conditions (all $t_{13} = 3.6–7.3$, $p = 0.004–10^{-6}$; Figure 4A, black rectangles). This theta synchronization was accompanied by an evoked response (i.e., a P1-N1-P2 complex, Figure S1A). More specific stimulus-based comparisons revealed that the stimulus-evoked theta synchronization after the onset of the noise increased significantly when the target contained a gap versus no gap. This gap-related increase appeared most consistently between ~100–400 ms relative to the onset of the noise. The earliest statistically detectable effects were found at ~150 ms in the ambiguous conditions (gap simple effects;

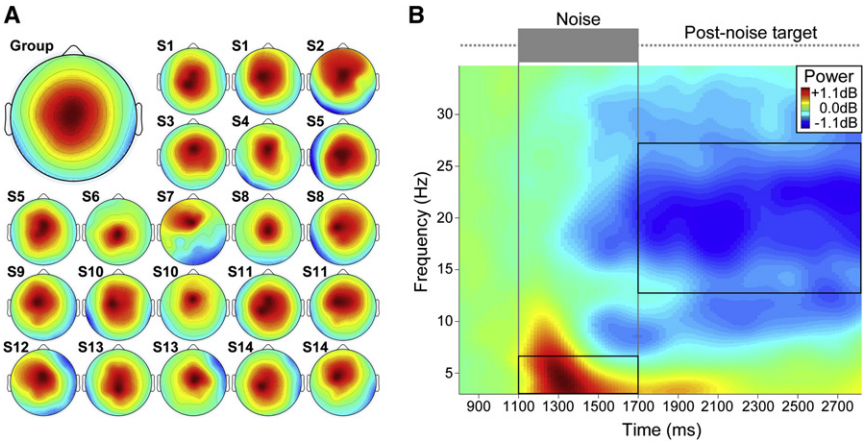


**Figure 3. Topographical-Functional Characteristics of Maximally Temporally Independent EEG Components**

(A) A component cluster (enlarged) showed EEG activities mainly projected to central-medial scalp sites, consistent with participants' individual components.

(B) The cluster further exhibited prominent theta-power increases (red: synchronization) locked to the onset of the noise (left vertical line) and sustained beta-power decreases (blue: desynchronization) locked to the offset of the noise (right vertical line) relative to the pre-noise interval. These power changes (see delineated time-frequency regions in the grand-mean spectrum) were further analyzed for effects of stimulus changes and restoration switches.

Figure 4B, red marks). The effects further reached their maximum at ~230 ± 50 ms averaged across all masking conditions. Averaged across the noise interval the gap-related increase was highly significant (gap main effect), in particular when the gap was fully unmasked (0.6-oct. condition: gap simple effect; Figures 4C and 6A). Theta synchronization further scaled with the spectral segregation between the target and the noise (i.e., with the masking parameter). This effect was significant for interrupted targets (masking effect), and a similar nonsignificant trend was observed for uninterrupted targets (no masking effect; Figures 4C and 6A). The stimulus differences evoked a consistent pattern of time-locked effects in the N1 response to the onset of the noise (latency: ~120 ms); P1 or P2 responses were not affected significantly (see Supplemental Data, Figures S1A, S1C, and S5A). Therefore, the temporal gap in the tone and the spectral gap in the noise evoked synchronization of theta oscillations after the gap's onset.

The gap also exerted significant influences after the interruption; these effects were reflected most strongly in desynchronization of beta (13–27 Hz) oscillations (see Supplemental Data, Figure S3 and S5C).

## Restoration-Related Effects on EEG Oscillations

The results so far show that acoustic gaps evoke synchronization of slow cortical oscillations that may encode these gaps especially after ~150 ms. To disentangle perceptual and acoustic influences, we next investigated restoration-related effects independently of physical stimulus effects (see Experimental Procedures). Strikingly, this restoration-based analysis revealed that the stimulus-evoked theta synchronization was significantly weaker when listeners reported hearing the continuity illusion versus the gap in the same stimulus (Figure 5). This restoration-related suppression evolved before the actual gap, reached significance during the gap, and continued after the gap. The earliest statistically detectable effect was found ~50 ms after the onset of the gap (0-oct. condition: restoration simple effect; Figure 5B, red marks). The effect further reached its maximum at ~170 ± 70 ms averaged across the ambiguous conditions. Averaged across the gap interval (Figure 5A, black rectangles), the suppression was highly significant (restoration main effect), especially when the gap was fully masked (0-oct. condition: restoration simple effect; Figures 5C and 6B). The effect was most significant on the synchronization of 3–4 Hz oscillations within the delta and theta range (Figure S2; see Experimental Procedures). Analysis of slow evoked activities revealed no significant restoration-related effect (see Supplemental Data, Figures S1B, S1C, and S5B). Therefore, the suppression of synchronization likely was induced at variable latencies across trials (Tallon-Baudry and Bertrand, 1999) and especially in 3–4 Hz oscillations. Notably, the induced restoration-related modulations were consistent with the gap-evoked modulations (Figure 4): illusory continuity was encoded as true continuity rather than true discontinuity during the gap.

Significant restoration-related modulations were observed also after the interruption; these effects were reflected in a suppression of beta desynchronization especially 600–900 ms after the gap (see Supplemental Data, Figure S4).

## Localization of Oscillatory EEG Sources Involved in Auditory Restoration

The locations of cortical EEG sources associated with restoration switches were identified using a cortically constrained distributed source analysis (see Experimental Procedures). This analysis revealed significant restoration-related modulations in theta synchronization in the right AC during the gap (restoration main effect, $t_9 = 3.6$, corrected $p < 0.05$; Figure 7B, left), consistent with our experimental hypothesis and the cluster-based results (see Supplemental Data). Left frontal sources exhibited similar nonsignificant modulations (Figure 7A, right). The most significant regions in the right AC encompassed the supratemporal plane, superior temporal gyrus (STG), and portions lateral to Heschl's gyrus (HG), including superior temporal sulcus and middle temporal gyrus. No significant masking effect or interaction could be detected in these regions. The regional peak was located on the middle portion of STG adjacent to lateral HG (Talairach coordinates in mm: x = 51, y = −27, z = 10) and, importantly, the location of this region of interest was compatible with the restoration-related region that we identified previously in the right primary AC using fMRI (restoration main effect, $t_{10} = 2.1$, uncorrected $p < 0.05$; Figure 7B, right). Analysis of source power time series in this region confirmed that illusory restorations versus true discontinuity percepts were associated with

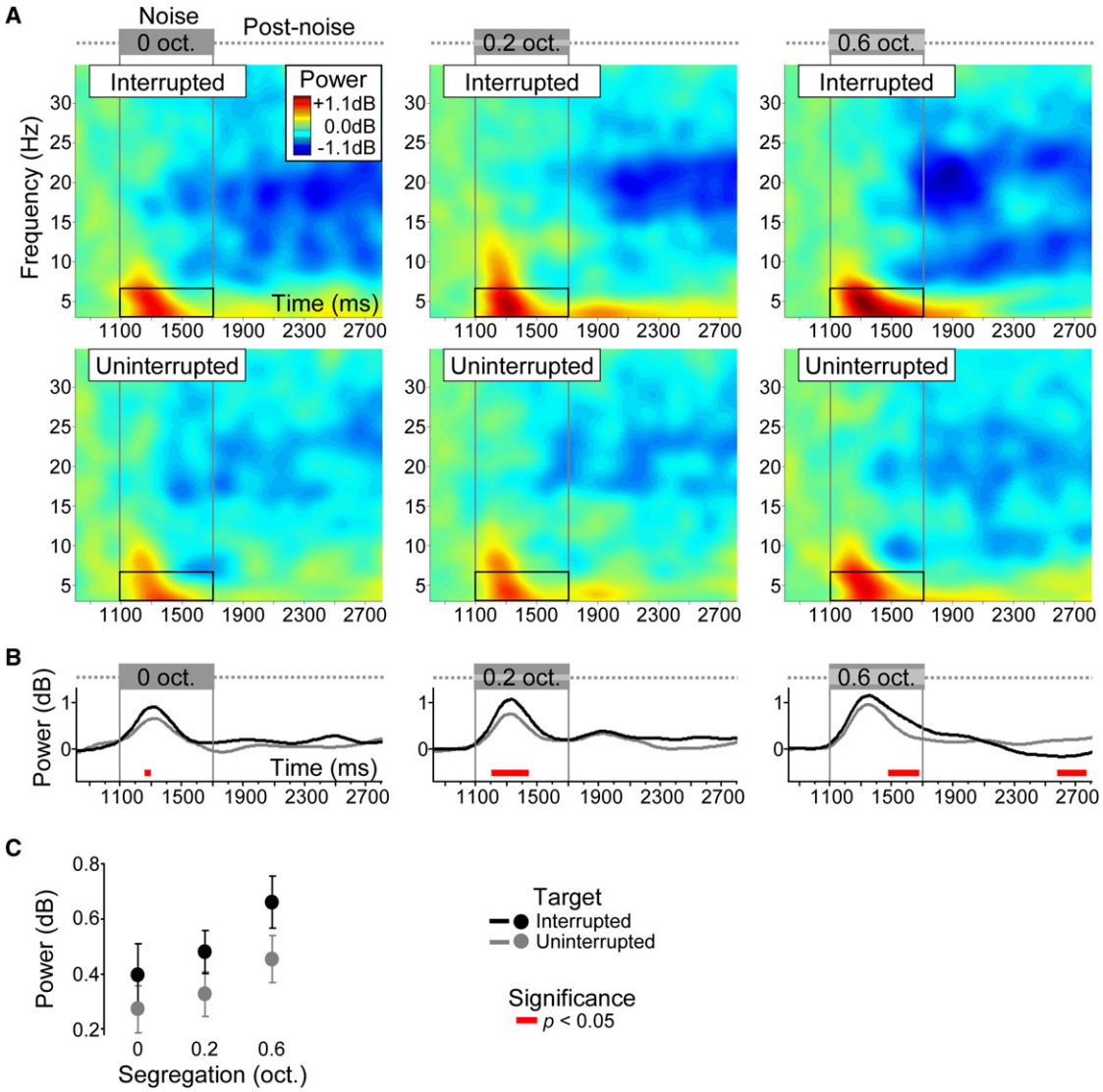


**Figure 4. Effects of Stimulus Changes on Theta EEG Power**

(A) The interrupted target (upper row) evoked stronger synchronization (red) of slow oscillations during the noise interval (black rectangle) compared to the uninterrupted target (lower row), as suggested by the power spectra in the different masking conditions (columns). Vertical lines, noise onsets and offsets; oct., octaves.

(B) The earliest statistically detectable effects of the gap on theta synchronization (red marks) in the ambiguous conditions were found ~150 ms after the gap's onset, as revealed by the power time series.

(C) Average theta synchronization in the noise interval increased significantly when the target comprised a gap or was unmasked. Error bars indicate standard error across listeners. The results indicate that the salience of acoustic gaps in sounds is encoded in the synchronization of cortical theta oscillations.

a suppression of theta synchronization that evolved before the gap and continued during and after the gap (Figure 7C). Statistical analysis for lateralization effects (see Experimental Procedures) further revealed that the restoration-related suppression of theta synchronization was significantly stronger in this region than in the homologous region in the left AC (restoration × laterality interaction, $F_{1,9} = 5.4$, $p < 0.05$; Figure S6).

True discontinuity ratings versus illusory continuity ratings were further associated with stronger desynchronization of beta oscillations in the right sensory-motor cortex ~600–900 ms after the gap (see Supplemental Data, Figure S7).

## DISCUSSION

Our results show that interruptions in tones boost cortical theta oscillations. Strikingly, this stimulus-evoked synchronization is (1) elevated when a tone comprises a true gap and (2) suppressed when the same interrupted tone is perceptually restored. The restoration-related and stimulus-independent suppression is strongest during illusorily filled gaps and also present before and after these gaps. The suppression is lateralized to primary-like regions in the right AC and induced most significantly in ~4 Hz oscillations. Our findings suggest that the

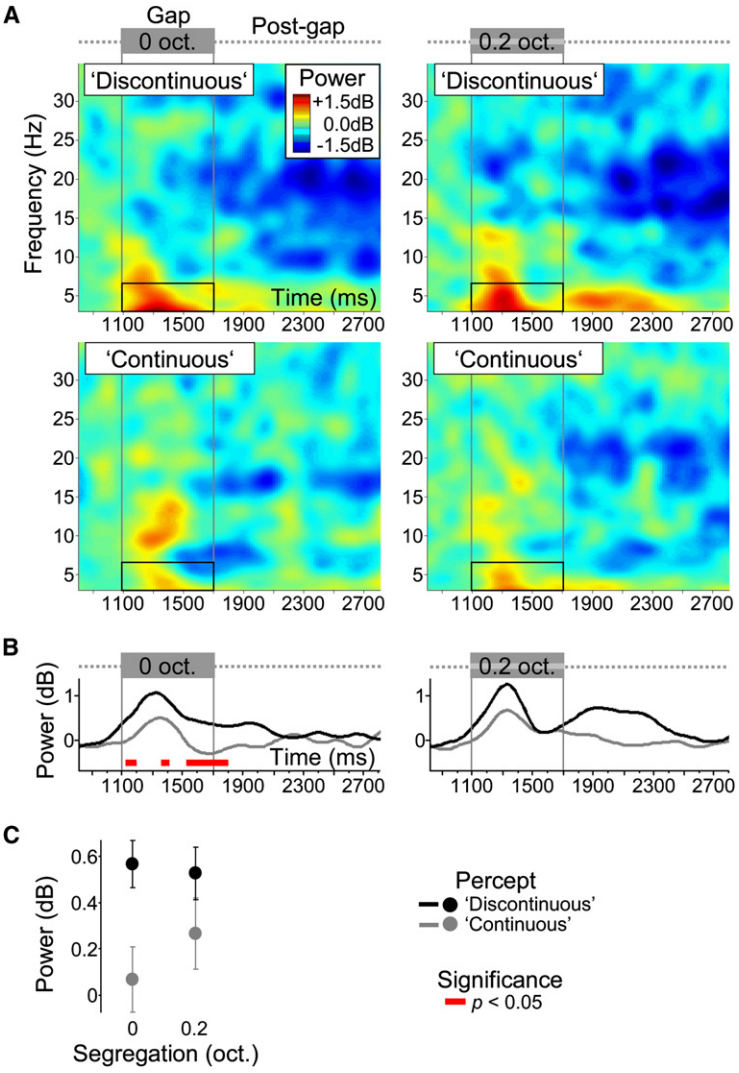


**Figure 5. Restoration-Related Effects on Theta EEG Power**

(A) Auditory restoration (lower row) was associated with suppression of slow oscillations during the gap compared to true discontinuity percepts of the same stimuli (upper row), as suggested by the power spectra in the ambiguous conditions (columns).

(B) The restoration-related suppression of stimulus-evoked theta synchronization evolved before the gap and continued during and after the gap; the earliest statistically detectable effect was found ~50 ms after the gap's actual onset (red marks).

(C) Average theta synchronization in the gap interval was significantly weaker when listeners restored the interrupted target. Error bars indicate standard error across listeners. The results indicate that auditory restoration is determined by a suppression of synchronization of cortical theta oscillations that are involved in the sensory encoding of acoustic gaps. For labels see Figure 4.

restoration of an interrupted sound is determined by suppression of synchronization of slow auditory-evoked cortical oscillations that are involved in the early encoding of auditory boundaries.

## Synchronization of Theta Oscillations and the Encoding of Acoustic Edges

We first found that interruptions in tones evoke significantly stronger synchronization of theta oscillations after ~150 ms when the sensory input comprises a gap versus no gap. This gap-evoked increase in synchronization further scales with the unmasking of gaps and therefore it may encode the salience of acoustic boundaries in cortical stimulus representations.

Analysis and synthesis of such boundaries or "edges" is integral to the formation of perceptual objects (Fishbach et al., 2001; Shamma, 2001), including illusorily restored sounds (Bregman, 1990; Nakajima et al., 2000). The underlying mechanisms may involve neurons in right AC that respond strongly to temporal edges in sounds (Herdener et al., 2007; Chait et al., 2008). Responses of such neurons typically are suppressed in right primary AC when temporal gaps are rendered less salient by masking noise (Petkov et al., 2007; Riecke et al., 2007; Heinrich et al., 2008). The present findings support these statements and propose that synchronization of theta oscillations in gap-encoding neurons may function as a cortical mechanism for representing boundaries of auditory objects.

We observed that the N1 response exhibits consistent gap-evoked increases, and therefore it may be coupled to the gap-evoked increases in theta synchronization (Grau et al., 2007). Similar modulations in scalp potentials have been associated with the detection of gaps in noise (Joutsiniemi et al., 1989; Pantev et al., 1996; Rupp et al., 2002; Heinrich et al., 2004; Michalewski et al., 2005; Pratt et al., 2005; Lister et al., 2007) and in noise-interrupted tones (Micheyl et al., 2003); these effects were observed reportedly around 120 ms and 150 ms after gaps' onset, respectively. The similar latency of these effects corroborates our N1 results and our interpretation that gap-evoked EEG modulations around 150 ms may encode salient acoustic boundaries.

In the literature, theta synchronization has been associated with the encoding of new sensory input, working memory, and increased task demands (for reviews see Klimesch, 1999; Kahana et al., 2001; Klimesch et al., 2008). Theta synchronization may occur during passive listening (Kolev et al., 2001) and can be enhanced by acoustic and cognitive factors such as stimulus salience and auditory attention (Yordanova and Kolev, 1998; Cacace and McFarland, 2003; McFarland and Cacace, 2004). The gap-evoked increases in theta synchronization that we observed thus could indicate also the sensory buffering of acoustic edges or attention shifts triggered by highly salient edges.

## Suppression of Theta Oscillations and the Restoration of Interrupted Sounds

Our main finding is that slow theta oscillations that appear to encode acoustic boundaries are suppressed during an interruption in a sound when that sound is illusorily restored. We found that this restoration-related suppression is most strongly induced in the right AC. While more specific localization in

**A**

| Factor | | Statistic | p-value |
|---|---|---|---|
| gap | 0-oct. condition | $t_{13} = -1.5$ | 0.2 |
| | **0.2-oct. condition** | $t_{13} = -2.3$ | 0.04 |
| | **0.6-oct. condition** | $t_{13} = -2.3$ | 0.04 |
| | **pooled masking conditions** | $F_{1,13} = 12.2$ | 0.004 |
| masking | **interrupted condition** | $F_{2,26} = 4.2$ | 0.03 |
| | uninterrupted condition | $F_{2,26} = 2.6$ | 0.09 |
| | **pooled gap conditions** | $F_{2,26} = 6.0$ | 0.008 |
| gap × masking interaction | | $F_{2,26} = 0.3$ | 0.8 |

**B**

| Factor | | Statistic | p-value |
|---|---|---|---|
| restoration | **0-oct. condition** | $t_{10} = 3.3$ | 0.008 |
| | 0.2-oct. condition | $t_{12} = 1.3$ | 0.2 |
| | **pooled masking conditions** | $F_{1,9} = 14.6$ | 0.005 |
| masking | 'discontinuous' condition | $t_9 = 0.7$ | 0.5 |
| | 'continuous' condition | $t_9 = -1.2$ | 0.3 |
| | pooled restoration conditions | $F_{1,9} = 0.5$ | 0.5 |
| restoration × masking interaction | | $F_{1,9} = 1.8$ | 0.2 |

**Figure 6. Statistical Results from Analyses of Average Theta EEG Power in the Noise Interval**

The analyses were based on stimulus changes (A) and restoration switches (B). Effects of factor "gap," "restoration," and "masking" were tested by comparing interrupted versus uninterrupted targets, "discontinuous" versus "continuous" ratings of the same interrupted target, and different masking conditions, respectively. Statistically significant effects are highlighted ($p < 0.05$).

primary versus secondary AC is limited by the spatial resolution of our EEG method, the location of the effect is highly similar to that of the restoration-related effect in right primary AC that we have identified previously using fMRI and the same stimuli and task as here (Riecke et al., 2007). Since theta EEG power and blood-oxygenation levels in human right primary AC may correlate (Mukamel et al., 2005), this functional-spatial match hints at corresponding mechanisms at early auditory cortical processing stages. The mechanisms may temporally integrate and perceptually analyze the sensory input given our result that restoration-related suppression of theta oscillations is strongest during the sensory encoding of illusorily filled gaps. Furthermore, the right-lateralization of the suppression may reflect that these mechanisms employ preferably long temporal integration windows in the right AC (~200 ms, corresponding to the period of theta oscillations) compared to those in the left AC, as proposed by current theories on functional lateralization in AC (Zatorre et al., 2002; Poeppel, 2003).

We observed weaker but consistent restoration-related modulations in frontal cortex, a region that is commonly

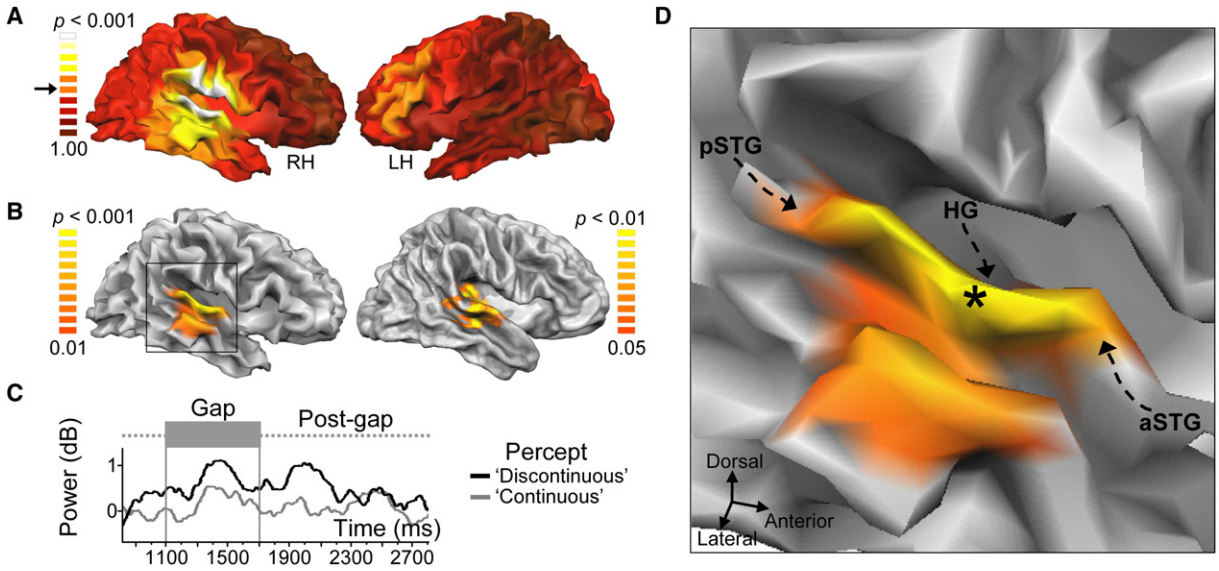


**Figure 7. Cortical Theta Sources Involved in Restoration Switches**

(A) Distributed cortical sources in right AC and left frontal cortex exhibited restoration-related modulations of stimulus-evoked theta synchronization. Brighter spots in the unthresholded maps reveal sources showing stronger modulations. Arrow: uncorrected $p < 0.05$; LH and RH: left and right hemisphere, respectively.

(B) The most significant restoration-related effects were localized in the right AC (left panel, D, corrected $p < 0.05$). Similarly localized restoration-related effects on blood oxygenation levels were identified previously in the right primary AC (right panel, uncorrected $p < 0.05$; adapted from Riecke et al., 2007).

(C) Restoration was associated with suppression of theta oscillations in right AC during and also around the gap compared to true discontinuity percepts of the same stimuli, as shown by the source power time series extracted from the regional peak (see asterisk in D).

(D) Enlarged view of right AC (rectangle in B) revealing the location of the restoration-related theta sources relative to major auditory cortical landmarks (pSTG, posterior superior temporal gyrus; HG, Heschl's gyrus; aSTG, anterior superior temporal gyrus). The results indicate that auditory restoration of interrupted sounds is associated with a suppression of evoked theta oscillations in primary-like regions in the right AC.

associated with theta oscillations (for reviews see Klimesch, 1999; Kahana et al., 2001). Frontal cortex has been shown to synchronize its activity with other cortical regions in the theta band during the mental processing of behaviorally relevant content. This synchronization has been attributed to top-down processing (Von Stein and Sarnthein, 2000) and therefore, the suppression of theta synchronization that we observed in AC could reflect feedback induced from higher task-related processing stages in frontal cortex. Furthermore, sensory input can propagate beyond AC within ~25 ms (Inui et al., 2006), so the emergence of significant suppressive effects on auditory cortical theta oscillations after ~50 ms is compatible with the existence of possible feedback signals from nonauditory regions.

Our result that restoration of interrupted sounds is accompanied by spontaneous suppression of stimulus-evoked oscillations indicates that the underlying mechanisms may depend on the *absence of synchronization* among gap-evoked neuronal oscillations. We also observed that this suppression is most significant in oscillations around the restored sound's amplitude modulation (AM) rate. Together, the results suggest that restoration of an interrupted sound depends on the suppression of neuronal phase-locking to that sound's acoustic structure, which could be an auditory cortical mechanism for blurring intelligibility (Luo and Poeppel, 2007). Using stimuli with varying AMs could allow establishing such sound structure-specificity of restoration mechanisms.

It is noteworthy that we observed consistent restoration-related modulations also in beta oscillations after illusorily filled gaps. This result confirms previously established findings showing that motor responses are preceded by desynchronization of beta oscillations (Pfurtscheller and Lopes da Silva, 1999; Kaiser et al., 2001, 2007; Alegre et al., 2003a, 2003b, 2004, 2006). The modulations likely affected hand-related preparatory signals, given that contralateral sensory-motor regions including the premotor cortex and parietal regions that may be relevant for nonillusory auditory grouping phenomena (Cusack, 2005) showed the strongest modulations. The modulations reached significance around 600 ms after the gap, so it can be concluded that by that time listeners had restored the interrupted sound and selected a response.

## Possible Origins of Switches in Theta Suppression and Restoration

The observed theta suppression in early AC was independent of physical stimulus changes and therefore it likely was induced by physiological intertrial variability in the proposed sensory-perceptual mechanisms. This variability could be caused by stochastic fluctuations in the neuronal activity evoked by the ambiguous noise maskers (Micheyl et al., 2005).

Alternatively, these fluctuations could be coupled to a very slow ongoing EEG oscillation as may be indicated by the slow build-up and decline of the suppression before and after illusorily filled gaps, respectively. Power modulations in theta EEG oscillations and switches in the detection of identical somatosensory stimuli at threshold have been associated previously with the phase of ongoing EEG oscillations at 0.01–0.1 Hz (Monto et al., 2008). These infraslow oscillations thus could influence also the sensory encoding of auditory stimuli and explain the relatively sustained theta power modulations and the restoration switches that we observed.

Another possible yet consistent origin of the intertrial fluctuations could be spontaneous changes in listeners' attention that have been found previously to control the selection and perceptual interpretation of acoustic-sensory features by modulating induced neuronal oscillations (for review see Engel and Singer, 2001), especially in the low-frequency range (Von Stein and Sarnthein, 2000; Von Stein et al., 2000; Buzsaki and Draguhn, 2004; Canolty et al., 2006; Lakatos et al., 2008; Schroeder and Lakatos, 2008, 2009; Bonte et al., 2009). When listeners happened to attend more to a gap, for example, the gap possibly was encoded as more salient; alternatively, when a gap was encoded as more salient it possibly attracted more attention. Each of these cases may explain the increases in theta synchronization that we found associated with true gap perception (see also Yordanova and Kolev, 1998; Cacace and McFarland, 2003; McFarland and Cacace, 2004). Furthermore, slow ongoing neuronal oscillations can phase-lock to an attended stimulus' presentation rate and thereby enhance neuronal responses evoked by that stimulus (Lakatos et al., 2005, 2007, 2008; Schroeder and Lakatos, 2008). Given these previous findings, the increases in theta synchronization that we observed could reflect spontaneous attention-related phase-locking of slow ongoing neuronal oscillations to the target's AM which enhanced the salience of gaps in stimulus representations.

To sum up, fluctuations in each of these factors could have modulated the sensory encoding of the auditory input and therewith determined the salience of gaps in cortical stimulus representations as well as the switches in perceptual stimulus interpretation that we observed. Since our methods were not set up for investigating infraslow oscillations (for example, see Vanhatalo et al., 2005; Monto et al., 2008) or manipulating listeners' attention, it remains a matter of debate whether and how exactly these factors contribute to fluctuations in theta oscillations and restoration, or to perceptual bistability in general (for discussions see Leopold and Logothetis, 1999; Pressnitzer and Hupe, 2006). Overall, our results clearly suggest that slow ongoing EEG oscillations in the right AC controlled the restoration of interrupted sounds by modulating slow theta oscillations especially during the sensory encoding of gaps.

## How and When Does Auditory Restoration Emerge in the Auditory System?

According to Bregman's (1990) prevailing view, restoration emerges from an early automatic process that extracts sensory features from acoustic input and from a later voluntary process that matches the extracted features with perceptual expectancies or schemas (for a recent review see Ciocca, 2008). To integrate the present and previous neurophysiologic and neuroimaging findings with this psychoacoustic framework, we propose a neural model for restoration (Figure 8). A central aspect of our model builds on the present evidence that flexible sensory-perceptual encoding of acoustic gaps in right AC may determine restoration.

When a gap in a sound is masked by noise (Figure 8A), the interrupted sound and the noise may evoke uninterrupted excitations in peripheral neurons (Delgutte, 1990) which swamp the

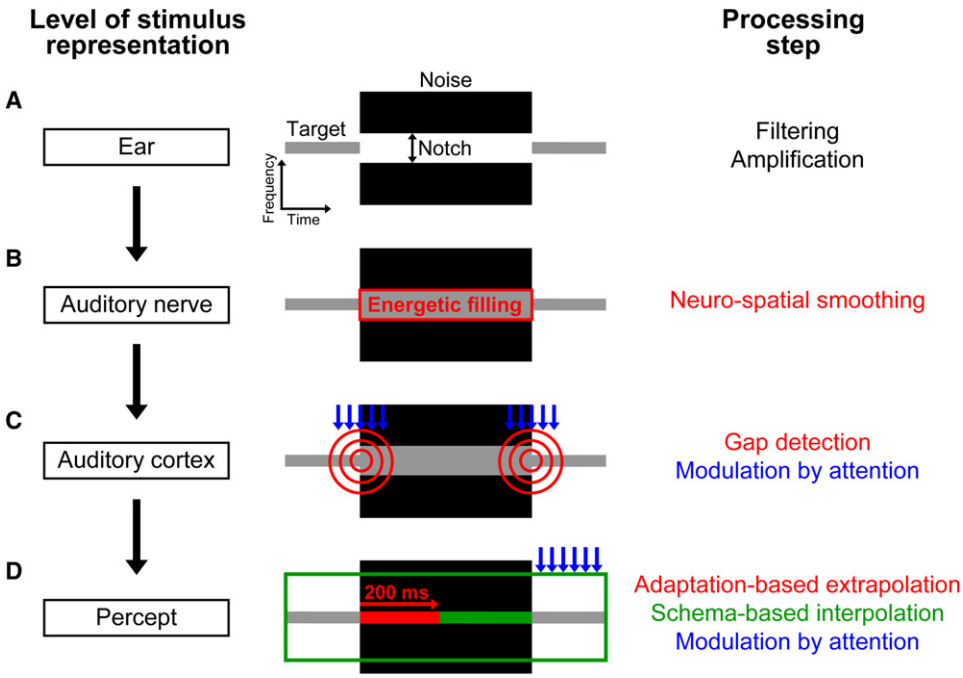


**Figure 8. Sketch of a Neural Model for Auditory Restoration**

(A) A temporal gap in an interrupted sound (target, gray bar) is masked partially by noise (black rectangle) comprising a spectral gap (notch).

(B) Peripheral auditory filters fill in sensory energy in the omitted critical band (gray rectangle) and smear the sensory stimulus representation.

(C) Auditory cortical neurons analyze the filled target band representation for gaps. The sensitivity of these neural edge detectors (red circles) is modulated, for example, by attention (blue arrows).

(D) When no gap is detected, adaptation facilitates buffering of the fading target sound for ~200 ms (red arrow), which temporarily extends the sound percept into the noise (red bar). Auditory cortical neurons comprising large spectrotemporal receptive fields (green rectangle) match the extrapolated target representation with learned perceptual patterns after the gap, which may lead to perceptual interpolation of the interrupted sound (green bar) depending on attention (blue arrows).

sensory evidence for the gap in the critical band (Figure 8B, red rectangle). Restoration may occur when neurons fail to detect sensory evidence for the gap around ~150 ms and thus represent the interrupted sound as uninterrupted (Warren et al., 1972; for review see Warren, 1999). As mentioned, populations of such neural gap detectors may exist in the right primary AC, and their sensitivity (Figure 8C, red circles) could be controlled already before the gap by modulating signals (Figure 8C, blue arrows), for example, those involved in allocating attention or organizing acoustic input (for reviews see Carlyon, 2004; Fritz et al., 2007a; Alain and Bernstein, 2008). The underlying mechanisms may involve a suppression of theta synchronization among these gap detectors (see Results, Figure 5) or a broadening of their receptive fields (Fritz et al., 2007b). Such mechanisms could "smooth out" flexibly the cortical representation of the gap and eliminate the identification of veridical object boundaries during the stimulus interval and the gap interval in particular.

The illusory extrapolation of the interrupted sound into the noise (Bregman, 1990; Figure 8D, red line) could be achieved by auditory cortical neurons that respond strongly to sustained sensory input (Petkov et al., 2007) or by neural mechanisms for forward masking (for review see Micheyl et al., 2007) or sensory memory (Ulanovsky et al., 2003). Such presumably automatic mechanisms may sample the acoustic regularities in the cortical stimulus representation in intervals of ~200 ms and match them to subsequent acoustic input (Näätänen et al., 2001; Micheyl et al., 2003). During gaps longer than ~200 ms, however, the extrapolated representation of the interrupted sound may be overwritten gradually by more recent sensory input (that is, by the ongoing noise) and accompanied by the fading of the sound's percept (Wrightson and Warren, 1981; Warren et al., 1994).

Later-operating mechanisms may then interpolate the fading sound representation by matching it with learned auditory patterns or perceptual expectancies (Repp, 1992) in auditory (Griffiths and Warren, 2002) or other cortical regions (Shahin et al., 2009). Such mechanisms may be modulated (Figure 8D, blue arrows) by auditory attention (Samuel and Ressler, 1986) or the auditory context (Sivonen et al., 2006; Riecke et al., 2009), and they might involve auditory cortical filters that can integrate sensory input across large, complex spectrotemporal windows (Figure 8D, green rectangle; Husain et al., 2005). Depending on this matching, the restoration of the interrupted sound could be completed within ~600 ms after the gap (see Results, Figure S4).

## Conclusions

The present findings add novel evidence to our understanding of the constructive nature of hearing. Perceptual restoration of interrupted sounds depends on spontaneous fluctuations in

the auditory system, which may be coupled to the listener's attention. These induced fluctuations attenuate the perceptual salience of gaps in sounds by suppressing their sensory encoding in the right AC. The suppressive effects evolve already before an illusorily filled gap and reach their maximum shortly after the gap's actual onset, as reflected by a significant suppression of stimulus-evoked synchronization of slow theta oscillations after ~50 ms. The restoration of the whole sound may be completed by around 600 ms after the gap. Conclusively, our data set constraints on the timing of auditory cortical mechanisms assumed to facilitate stable hearing in noisy environments and provide a neural model that may inform the development of improved assisted hearing devices.

## EXPERIMENTAL PROCEDURES

### Stimuli

A schematic auditory scene was assembled of sine-modulated tones (targets; duration: 2800 ms, carrier frequency: 930 Hz, AM rate: 3 Hz) and band-passed white noise (duration: 600 ms, bandwidth: 2 oct.) centered on the tone (Figure 1A). For the interrupted target, the offsets and onsets of the gap and the noise were synchronized. The uninterrupted target was acoustically matched except that no gap was inserted. The noise was band-stopped at the target's carrier frequency. To parameterize the masking of the gap, the spectral segregation of the target band from the noise (defined as the half spectral gap width) was varied across three levels (Figure 1B). Noise and stimuli were equated on their root mean square amplitudes, respectively. Onsets and offsets of targets and noise were linearly ramped with 3 ms rise-fall times. Stimuli were sampled at 44.1 kHz with 16 bit resolution using Matlab. Stimuli were presented diotically at 70 dB sound pressure level (SPL) using Presentation 9.30 software, a Creative Sound Blaster Audigy 2ZS sound card, and JB Control 25 speakers.

### Participants, Design, and Task

Fourteen volunteers (age: 26 ± 4 years, mean ± standard deviation) who reported normal hearing and motor abilities participated in the study after providing informed consent. The local ethical committee (Ethische Commissie Psychologie) approved the procedure. Participants were seated in a comfortable chair in an electrically shielded and sound-attenuated room. Their ability to hear continuity illusions and perform the task (see next paragraph) was assessed in 75 training trials. Restoration thresholds were estimated based on the method of limits (see Supplemental Experimental Procedures). These thresholds were implemented as intermediate levels of the masking parameter (Figure 1B; segregation: 0.2 ± 0.1 oct.) to define individual ambiguous conditions expected to evoke bistable percepts.

In the subsequent EEG experiment, participants performed a forced-choice delayed-response task. Trials comprised stimulation and response intervals indexed by a fixation cross changing in color (Figure 1C). Response intervals were dissociated from stimulus intervals by silent intervals of 1.5 s so that motor responses did not interfere with auditory-evoked EEG signals. Participants were instructed on an LCD screen to attend to targets during stimulus intervals and to rate their perceived continuity on a four-point scale. Ratings were performed during the delayed response intervals by pressing a button with either the left hand (buttons "most likely discontinuous" and "likely discontinuous") or right hand (buttons "likely continuous" and "most likely continuous") using the middle or index finger (respectively). Participants were further instructed to fixate and to delay eye blinks or other movements to response intervals. The six experimental conditions were presented in randomized order in blocks of 35 s duration using a jittered interstimulus interval of 2–2.5 s to reduce expectations of listeners. In total 80 blocks (480 trials) were presented pseudorandomly so that successive trials always differed. Participants were permitted to take breaks every 16 blocks.

### EEG Recording and Data Processing

EEG was measured with 61 Ag/AgCl scalp electrodes at equidistant positions (Easycap) relative to a left mastoid reference electrode. Interelectrode impedances were kept below 5 kΩ by abrading the scalp. Electrooculography (EOG) was monitored using an electrode placed below the left eye. Individual electrode locations relative to fiducials (nasion, preauricular marks) were recorded using a 3D digitizer (Zebris). EEG data were recorded with Neuroscan SynAmps using an analog pass band of 0.05–70 Hz (filter slopes −12 dB/oct.). After digitization (sampling rate 250 Hz, resolution 0.168 μV/bit) data were processed using the EEGLAB toolbox (Delorme and Makeig, 2004) and custom Matlab scripts. After high-pass filtering (cutoff: 1 Hz) data were rereferenced to an average reference based on the mean activity of all channels and 4.5 s epochs including a 1 s prestimulus interval were extracted.

Single data channels showing artifacts related to poor skin contacts were excluded from further analysis (two channels per data set on average). Trials containing nonrepetitive movement artifacts were identified semiautomatically using a ± 75 μV criterion and visual inspection. Trials during which participants were not engaged actively in the task were identified based on lapsed button responses. Both types of trials were discarded, resulting in individually single-trial artifact-cleaned data sets comprising 386 ± 26 trials (~750 samples per trial per channel). Trials affected by blinks, eye movements, or other repetitive artifacts were not discarded, as the underlying processes could be separated from brain-related EEG processes using independent component analysis (ICA) as follows. The single-trial artifact-cleaned data sets were decomposed into linear sums of 59 ± 2 spatially fixed and maximally temporally ICs using the Infomax ICA algorithm as implemented in EEGLAB (*runica*, see Makeig et al., 1997; Lee et al., 2000). ICs primarily accounting for blinks or eye movements were identified based on their frontal scalp distributions and their irregular occurrences across trials. Remaining artifacts were identified based on their nondipolar scalp maps, flat activity spectra, and irregular occurrences (Jung et al., 2000a, 2000b; Delorme et al., 2007). Removal of these ICs resulted in individually pruned artifact-cleaned datasets comprising 12 ± 5 ICs.

### Computation of EEG Power Spectra

#### *EEG Component Cluster Spectra*

EEG component power spectra were computed from time-frequency analysis by sliding an 1100 ms window across the single-trial activity time series. The number of cycles per Morlet wavelet was increased linearly from 3 to 17.5 across the investigated frequency range (3–35 Hz). Mean event-related spectral power changes were estimated relative to the mean spectrum in the 500 ms pre-noise interval (baseline) on a logarithmic scale for each frequency band.

Individual ICs were clustered based on similarities in their scalp topographies, spectra, and evoked waveforms using a clustering algorithm implemented in EEGLAB (see Supplemental Experimental Procedures). A component cluster whose distinctive features were most suggestive of auditory cortical processes was selected for further analysis. This cluster showed central-medial activities (Figure 3A) that likely reflected synchronous bilateral auditory cortical processes that were merged into a single component due to their temporal dependencies (Makeig et al., 1997). Theta oscillations in this cluster exhibited the strongest time locking (Figure 3B), which is compatible with auditory cortical processes.

Subsequent random-effects analyses of this cluster were focused on specific time-frequency windows of interest. These windows were dimensioned based on the grand-mean cluster spectrum such that they included the EEG frequency bands (theta: 3–7 Hz and beta: 13–27 Hz) and stimulus intervals (noise interval and post-noise interval) that were modulated most strongly by the task. For more specific narrow band analyses within the delta (1–2 Hz) and theta range, 1 Hz wide windows were used after power was estimated relative to the 1000 ms pre-noise interval using one cycle per wavelet. The windows remained fixed across participants and conditions unless otherwise stated. For each participant and condition, a mean cluster spectrum was computed by averaging across the respective component spectra (the individual clusters comprised 7 ± 3 ICs). Mean cluster power was estimated in each condition by averaging across all power estimates within the time frequency window of interest. These mean power measures were well-fitted

with normal distributions as assessed by Lilliefors tests, permitting their analysis with parametric statistical tests (Kiebel et al., 2005).

#### *Cortically Constrained Distributed EEG Source Analysis*

Cortical EEG sources were localized using a cortically constrained distributed inverse model based on the minimum L2-norm approach (Dale and Sereno, 1993; Dale et al., 2000; Lin et al., 2004; 2006a, 2006b; Esposito et al., 2009a, 2009b). For each participant, the activity time-series of the artifact-cleaned and unclustered ICs were projected back onto the individual scalp electrode locations. The single-trial channel data were filtered using a continuous wavelet transform (CWT; Tallon-Baudry and Bertrand, 1999) whose center frequency and wavelet ratio were set such that the frequency band of interest was passed (theta: 5 Hz and 5; beta: 21 Hz and 21, respectively). The individually digitized electrode locations were fitted to a scalp model reconstructed from T1-weighted magnetic resonance images of the MNI-152 template head (Montreal Neurological Institute). Cortically constrained sources were defined by vertices of a cortical surface mesh that was extracted from the same template images (Esposito et al., 2009a). The CWT-filtered scalp channel data were projected onto these sources as single-trial source power time series using individually estimated and noise-normalized minimum-norm inverse solutions (Esposito et al., 2009a, 2009b; see Supplemental Experimental Procedures). All computations were performed using plug-ins programmed specifically for BrainVoyager QX version 1.10 software (Brain Innovation, Maastricht, The Netherlands).

Statistical tests were performed at each vertex of the cortex mesh and for the same time windows as in cluster analysis. For each participant, statistical t maps first were computed for each experimental condition to assess differences in mean source power during the interval of interest versus the baseline interval. The t statistics then were standardized to z scores and the z maps were smoothed spatially along the cortex mesh (one iteration of a nearest-neighbor averaging operation) to compensate for anatomical intersubject variability. The resulting z maps of all individual subjects and conditions were forwarded to the same random-effects analyses as the IC-clustered data (see Statistical Analyses).

To enable analysis of lateralization effects, potentially homologous left-sided vertices were defined on the cortex mesh by first reversing the x axis coordinate of the right-sided vertex that exhibited the most significant main effect (Figure 7D, asterisk) and then including adjacent vertices within a radius of 10 mm.

### Statistical Analyses

Mean EEG power was analyzed for stimulus effects and restoration-related effects using two orthogonal tests. First, effects of the acoustic gaps were assessed by analyzing differences between interrupted and uninterrupted target conditions and their modulations by the masking parameter. This *stimulus-based* analysis involved a 2 × 3 analysis of variance (ANOVA) for repeated-measures, including two levels of "gap" (interrupted, uninterrupted) and three levels of "masking" (0, 0.2, 0.6 oct.) as fixed factors and "listener" as a random factor. The same model was used for analyzing participants' continuity rating data.

Second, effects related to auditory restoration were determined by comparing identical stimulus conditions in which listeners had rated the interrupted target "continuous" versus "discontinuous." For this *restoration-based* and stimulus-independent analysis, trials from the rating condition that occurred more frequently were randomly rejected so that both rating conditions were matched for number of trials, separately for each ambiguous condition (outlined in black in Figure 1B) and for each listener. Significance of restoration-related effects was assessed with paired t tests across listeners who switched their illusory ratings most frequently and thus provided the most samples (Figure 2B). Interactions and main effects were tested using a 2 × 2 ANOVA including two levels of "restoration" ("continuous," "discontinuous") and two levels of "masking" (0, 0.2 oct.) as fixed factors, and "listener" (n = 10) as a random factor.

Both analyses were applied to the IC-clustered data and the *restoration-based* analysis was applied also to the unclustered IC data in source space. Random-effect t maps resulting from source analyses were corrected for multiple comparisons using a spatial cluster criterion (see Supplemental Experimental Procedures). For testing the lateralization of main effects on source power, z scores were extracted and averaged across the sources of interest per hemisphere, and submitted to a 2 × 2 × 2 (restoration × masking × laterality) ANOVA for repeated-measures (n = 10).

## SUPPLEMENTAL DATA

Supplemental Data include Supplemental Experimental Procedures, Supplemental Discussion, and seven figures and can be found with this article online at http://www.cell.com/neuron/supplemental/S0896-6273(09)00845-9.

## ACKNOWLEDGMENTS

This work was supported by the Netherlands Organization for Scientific Research (NWO) Cognitie programma grant 05104020 and VIDI 45204330. We thank Hanna Renvall and Alexander Gutschalk for useful comments on the study, Anke Walter for help with data acquisition, Federico De Martino for advice on time-frequency analysis, and Claudia Schreiner, Daniel Mendelsohn, and three anonymous reviewers for constructive comments on the manuscript.

Accepted: October 5, 2009
Published: November 25, 2009

## REFERENCES

Alain, C., and Bernstein, L.J. (2008). From sounds to meaning: the role of attention during auditory scene analysis. Curr. Opin. Otolaryngol. Head Neck Surg. *16*, 485–489.

Alegre, M., Gurtubay, I.G., Labarga, A., Iriarte, J., Malanda, A., and Artieda, J. (2003a). Alpha and beta oscillatory changes during stimulus-induced movement paradigms: effect of stimulus predictability. Neuroreport *14*, 381–385.

Alegre, M., Labarga, A., Gurtubay, I.G., Iriarte, J., Malanda, A., and Artieda, J. (2003b). Movement-related changes in cortical oscillatory activity in ballistic, sustained and negative movements. Exp. Brain Res. *148*, 17–25.

Alegre, M., Gurtubay, I.G., Labarga, A., Iriarte, J., Valencia, M., and Artieda, J. (2004). Frontal and central oscillatory changes related to different aspects of the motor process: a study in go/no-go paradigms. Exp. Brain Res. *159*, 14–22.

Alegre, M., Imirizaldu, L., Valencia, M., Iriarte, J., Arcocha, J., and Artieda, J. (2006). Alpha and beta changes in cortical oscillatory activity in a go/no go randomly-delayed-response choice reaction time paradigm. Clin. Neurophysiol. *117*, 16–25.

Bonte, M., Valente, G., and Formisano, E. (2009). Dynamic and task-dependent encoding of speech and voice by phase reorganization of cortical oscillations. J. Neurosci. *29*, 1699–1706.

Braaten, R.F., and Leary, J.C. (1999). Temporal induction of missing birdsong segments in European starlings. Psychol. Sci. *10*, 162–166.

Bregman, A.S. (1990). Auditory Scene Analysis: The Perceptual Organization of Sound (Cambridge, MA: MIT Press).

Buzsaki, G., and Draguhn, A. (2004). Neuronal oscillations in cortical networks. Science *304*, 1926–1929.

Cacace, A.T., and McFarland, D.J. (2003). Spectral dynamics of electroencephalographic activity during auditory information processing. Hear. Res. *176*, 25–41.

Canolty, R.T., Edwards, E., Dalal, S.S., Soltani, M., Nagarajan, S.S., Kirsch, H.E., Berger, M.S., Barbaro, N.M., and Knight, R.T. (2006). High gamma power is phase-locked to theta oscillations in human neocortex. Science *313*, 1626–1629.

Carlyon, R.P. (2004). How the brain separates sounds. Trends Cogn. Sci. *8*, 465–471.

Chait, M., Poeppel, D., and Simon, J.Z. (2008). Auditory temporal edge detection in human auditory cortex. Brain Res. *1213*, 78–90.

Ciocca, V. (2008). The auditory organization of complex sounds. Front. Biosci. *13*, 148–169.

Ciocca, V., and Bregman, A.S. (1987). Perceived continuity of gliding and steady-state tones through interrupting noise. Percept. Psychophys. *42*, 476–484.

Cusack, R. (2005). The intraparietal sulcus and perceptual organization. J. Cogn. Neurosci. *17*, 641–651.

Dale, A.M., and Sereno, M.I. (1993). Improved localization of cortical activity by combining EEG and MEG with MRI cortical surface reconstruction: a linear approach. J. Cogn. Neurosci. *5*, 162–176.

Dale, A.M., Liu, A.K., Fischl, B.R., Buckner, R.L., Belliveau, J.W., Lewine, J.D., and Halgren, E. (2000). Dynamic statistical parametric mapping: combining fMRI and MEG for high-resolution imaging of cortical activity. Neuron *26*, 55–67.

Delgutte, B. (1990). Physiological mechanisms of psychophysical masking: observations from auditory-nerve fibers. J. Acoust. Soc. Am. *87*, 791–809.

Delorme, A., and Makeig, S. (2004). EEGLAB: an open source toolbox for analysis of single-trial EEG dynamics including independent component analysis. J. Neurosci. Methods *134*, 9–21.

Delorme, A., Sejnowski, T.J., and Makeig, S. (2007). Enhanced detection of artifacts in EEG data using higher-order statistics and independent component analysis. Neuroimage *34*, 1443–1449.

Engel, A.K., and Singer, W. (2001). Temporal binding and the neural correlates of sensory awareness. Trends Cogn. Sci. *5*, 16–25.

Esposito, F., Mulert, C.F., and Goebel, R. (2009a). Combined distributed source and single-trial EEG-fMRI modeling: application to effortful decision making processes. Neuroimage *47*, 112–121.

Esposito, F., Aragri, A., Piccoli, T., Tedeschi, G., Goebel, R., and Di Salle, F. (2009b). Distributed analysis of simultaneous EEG-fMRI time-series: modeling and interpretation issues. Magn. Reson. Imaging *27*, 1120–1130.

Fishbach, A., Nelken, I., and Yeshurun, Y. (2001). Auditory edge detection: a neural model for physiological and psychoacoustical responses to amplitude transients. J. Neurophysiol. *85*, 2303–2323.

Fritz, J.B., Elhilali, M., David, S.V., and Shamma, S. (2007a). Auditory attention – Focusing the searchlight on sound. Curr. Opin. Neurobiol. *17*, 437–455.

Fritz, J.B., Elhilali, M., David, S.V., and Shamma, S. (2007b). Does attention play a role in dynamic receptive field adaptation to changing acoustic salience in A1? Hear. Res. *229*, 186–203.

Grau, C., Fuentemilla, L., and Marco-Pallarés, J. (2007). Functional neural dynamics underlying auditory event-related N1 and N1 suppression response. Neuroimage *36*, 522–531.

Griffiths, T.D., and Warren, J.D. (2002). The planum temporale as a computational hub. Trends Neurosci. *25*, 348–353.

Heinrich, A., Alain, C., and Schneider, B. (2004). Within- and between-channel gap detection in the human auditory cortex. Neuroreport *15*, 2051–2056.

Heinrich, A., Carlyon, R.P., Davis, M.H., and Johnsrude, I.S. (2008). Illusory vowels resulting from perceptual continuity: a functional magnetic resonance imaging study. J. Cogn. Neurosci. *20*, 1737–1752.

Herdener, M., Esposito, F., Di Salle, F., Lehmann, C., Bach, D.R., Scheffler, K., and Seifritz, E. (2007). BOLD correlates of edge detection in human auditory cortex. Neuroimage *36*, 194–201.

Houtgast, T. (1972). Psychophysical evidence for lateral inhibition in hearing. J. Acoust. Soc. Am. *51*, 1885–1894.

Husain, F.T., Lozito, T.P., Ulloa, A., and Horwitz, B. (2005). Investigating the neural basis of the auditory continuity illusion. J. Cogn. Neurosci. *17*, 1275–1292.

Inui, K., Okamoto, H., Miki, K., Gunji, A., and Kakigi, R. (2006). Serial and parallel processing in the human auditory cortex: A magnetoencephalographic study. Cereb. Cortex *16*, 18–30.

Joutsiniemi, S.L., Hari, R., and Vilkman, V. (1989). Cerebral magnetic responses to noise bursts and pauses of different durations. Audiology *28*, 325–333.

Jung, T.P., Makeig, S., Westerfield, M., Townsend, J., Courchesne, E., and Sejnowski, T.J. (2000a). Removal of eye activity artifacts from visual event-related potentials in normal and clinical subjects. Clin. Neurophysiol. *111*, 1745–1758.

Jung, T.P., Makeig, S., Humphries, C., Lee, T.W., McKeown, M.J., Iragui, V., and Sejnowski, T.J. (2000b). Removing electroencephalographic artifacts by blind source separation. Psychophysiology *37*, 163–178.

Kahana, M.J., Seelig, D., and Madsen, J.R. (2001). Theta returns. Curr. Opin. Neurobiol. *11*, 739–744.

Kaiser, J., Birbaumer, N., and Lutzenberger, W. (2001). Event-related beta desynchronization indicates timing of response selection in a delayed- response paradigm in humans. Neurosci. Lett. *312*, 149–152.

Kaiser, J., Lennert, T., and Lutzenberger, W. (2007). Dynamics of oscillatory activity during auditory decision making. Cereb. Cortex *17*, 2258–2267.

Kiebel, S.J., Tallon-Baudry, C., and Friston, K.J. (2005). Parametric analysis of oscillatory activity as measured with EEG/MEG. Hum. Brain Mapp. *26*, 170–177.

Klimesch, W. (1999). EEG alpha and theta rhythmicities reflect cognitive and memory performance: a review and analysis. Brain Res. Brain Res. Rev. *29*, 169–195.

Klimesch, W., Freunberger, R., Sauseng, P., and Gruber, W. (2008). A short review of slow phase synchronization and memory: Evidence for control processes in different memory systems? Brain Res. *1235*, 31–44.

Kolev, V., Rosso, O.A., and Yordanova, J. (2001). A transient dominance of theta ERP component characterizes passive auditory processing: evidence from a developmental study. Neuroreport *13*, 2791–2796.

Lakatos, P., Shah, A.S., Knuth, K.H., Ulbert, I., Karmos, G., and Schroeder, C.E. (2005). An oscillatory hierarchy controlling neuronal excitability and stimulus processing in the auditory cortex. J. Neurophysiol. *94*, 1904–1911.

Lakatos, P., Chen, C.M., O'Connell, M.N., Mills, A., and Schroeder, C.E. (2007). Neuronal oscillations and multisensory interaction in primary auditory cortex. Neuron *53*, 279–292.

Lakatos, P., Karmos, G., Mehta, A.D., Ulbert, I., and Schroeder, C.E. (2008). Entrainment of neuronal oscillations as a mechanism of attentional selection. Science *320*, 110–113.

Lee, T.W., Girolami, M., Bell, A.J., and Sejnowski, T.J. (2000). A unifying information-theoretic framework for independent component analysis. Comput. Math. Appl. *39*, 1–21.

Leopold, D.A., and Logothetis, N.K. (1999). Multistable phenomena: Changing views in perception. Trends Cogn. Sci. *3*, 254–264.

Lin, F.H., Witzel, T., Hämäläinen, M.S., Dale, A.M., Belliveau, J.W., and Stufflebeam, S.M. (2004). Spectral spatiotemporal imaging of cortical oscillations and interactions in the human brain. Neuroimage *23*, 582–595.

Lin, F.H., Belliveau, J.W., Dale, A.M., and Hämäläinen, M.S. (2006a). Distributed current estimates using cortical orientation constraints. Hum. Brain Mapp. *27*, 1–13.

Lin, F.H., Witzel, T., Ahlfors, S.P., Stufflebeam, S.M., Belliveau, J.W., and Hämäläinen, M.S. (2006b). Assessing and improving the spatial accuracy in MEG source localization by depth-weighted minimum-norm estimates. Neuroimage *31*, 160–171.

Lister, J.J., Maxfield, N.D., and Pitt, G.J. (2007). Cortical evoked response to gaps in noise: within-channel and across-channel conditions. Ear Hear. *28*, 862–878.

Luo, H., and Poeppel, D. (2007). Phase patterns of neuronal responses reliably discriminate speech in human auditory cortex. Neuron *54*, 1001–1010.

Makeig, S., Jung, T.P., Bell, A.J., Ghahremani, D., and Sejnowski, T.J. (1997). Blind separation of auditory event-related brain responses into independent components. Proc. Natl. Acad. Sci. USA *94*, 10979–10984.

McFarland, D.J., and Cacace, A.T. (2004). Separating stimulus-locked and unlocked components of the auditory event-related potential. Hear. Res. *193*, 111–120.

Michalewski, H.J., Starr, A., Nguyen, T.T., Kong, Y.Y., and Zeng, F.G. (2005). Auditory temporal processes in normal-hearing individuals and in patients with auditory neuropathy. Clin. Neurophysiol. *116*, 669–680.

Micheyl, C., Carlyon, R.P., Shtyrov, Y., Hauk, O., Dodson, T., and Pullvermüller, F. (2003). The neurophysiological basis of the auditory continuity illusion: A mismatch negativity study. J. Cogn. Neurosci. *15*, 747–758.

Micheyl, C., Tian, B., Carlyon, R.P., and Rauschecker, J.P. (2005). Perceptual organization of tone sequences in the auditory cortex of awake macaques. Neuron *48*, 139–148.

Micheyl, C., Carlyon, R.P., Gutschalk, A., Melcher, J.R., Oxenham, A.J., Rauschecker, J.P., Tian, B., and Wilson, E.C. (2007). The role of auditory cortex in the formation of auditory streams. Hear. Res. *229*, 116–131.

Miller, G.A., and Licklider, J.C.R. (1950). The intelligibility of interrupted speech. J. Acoust. Soc. Am. *22*, 167–173.

Miller, C.T., Dibble, E., and Hauser, M.D. (2001). Amodal completion of acoustic signals by a nonhuman primate. Nat. Neurosci. *4*, 783–784.

Monto, S., Palva, S., Voipio, J., and Palva, J.M. (2008). Very slow EEG fluctuations predict the dynamics of stimulus detection and oscillation amplitudes in humans. J. Neurosci. *28*, 8268–8272.

Mukamel, R., Gelbard, H., Arieli, A., Hasson, U., Fried, I., and Malach, R. (2005). Coupling between neuronal firing, field potentials, and fMRI in human auditory cortex. Science *309*, 951–954.

Näätänen, R., Tervaniemi, M., Sussman, E., Paavilainen, P., and Winkler, I. (2001). 'Primitive intelligence' in the auditory cortex. Trends Neurosci. *24*, 283–288.

Nakajima, Y., Sasaki, T., Kanafuka, K., Miyamoto, A., Remijn, G., and ten Hoopen, G. (2000). Illusory recouplings of onsets and terminations of glide tone components. Percept. Psychophys. *62*, 1413–1425.

Pantev, C., Eulitz, C., Hampson, S., Ross, B., and Roberts, L.E. (1996). The auditory evoked "off" response: sources and comparison with the "on" and the "sustained" responses. Ear Hear. *17*, 255–265.

Petkov, C.I., O'Connor, K.N., and Sutter, M.L. (2003). Illusory sound perception in macaque monkeys. J. Neurosci. *23*, 9155–9161.

Petkov, C.I., O'Connor, K.N., and Sutter, M.L. (2007). Encoding of illusory continuity in primary auditory cortex. Neuron *54*, 153–165.

Pfurtscheller, G., and Lopes da Silva, F.H. (1999). Event-related EEG/MEG synchronization and desynchronization: basic principles. Clin. Neurophysiol. *110*, 1842–1857.

Poeppel, D. (2003). The analysis of speech in different temporal integration windows: Cerebral lateralization as 'asymmetric sampling in time'. Speech Commun. *41*, 245–255.

Pratt, H., Bleich, N., and Mittelman, N. (2005). The composite N1 component to gaps in noise. Clin. Neurophysiol. *116*, 2648–2663.

Pressnitzer, D., and Hupe, J.M. (2006). Temporal dynamics of auditory and visual bistability reveal common principles of perceptual organization. Curr. Biol. *16*, 1351–1357.

Repp, B.H. (1992). Perceptual restoration of a 'missing' speech sound: auditory induction or illusion? Percept. Psychophys. *51*, 14–32.

Riecke, L., Van Opstal, J., Goebel, R., and Formisano, E. (2007). Hearing illusory sounds in noise: Sensory-perceptual transformations in primary auditory cortex. J. Neurosci. *27*, 12684–12689.

Riecke, L., Van Opstal, A.J., and Formisano, E. (2008). The auditory continuity illusion: A parametric investigation and filter model. Percept. Psychophys. *70*, 1–12.

Riecke, L., Mendelsohn, D., Schreiner, C., and Formisano, E. (2009). The continuity illusion adapts to the auditory scene. Hear. Res. *247*, 71–77.

Rupp, A., Gutschalk, A., Hack, S., and Scherg, M. (2002). Temporal resolution of the human primary auditory cortex in gap detection. Neuroreport *13*, 2203–2207.

Samuel, A.G., and Ressler, W.H. (1986). Attention within auditory word perception: Insights from the phonemic restoration illusion. J. Exp. Psychol. Hum. Percept. Perform. *12*, 70–79.

Schreiner, C. (1980). Encoding of alternating acoustical signals in the medial geniculate body of guinea pigs. Hear. Res. *3*, 265–278.

Schroeder, C.E., and Lakatos, P. (2008). Low-frequency neuronal oscillations as instruments of sensory selection. Trends Neurosci. *32*, 9–18.

Schroeder, C.E., and Lakatos, P. (2009). The gamma oscillation: master or slave? Brain Topogr. *22*, 24–26.

Shahin, A.J., Bishop, C.W., and Miller, L.M. (2009). Neural mechanisms for illusory filling-in of degraded speech. Neuroimage *44*, 1133–1143.

Shamma, S. (2001). On the role of space and time in auditory processing. Trends Cogn. Sci. *5*, 340–348.

Sivonen, P., Maess, B., Lattner, S., and Friederici, A.D. (2006). Phonemic restoration in a sentence context: Evidence from early and later ERP effects. Brain Res. *1121*, 177–189.

Sugita, Y. (1997). Neuronal correlates of auditory induction in the cat cortex. Neuroreport *8*, 1155–1159.

Tallon-Baudry, C., and Bertrand, O. (1999). Oscillatory gamma activity in humans and its role in object representation. Trends Cogn. Sci. *3*, 151–162.

Ulanovsky, N., Las, L., and Nelken, I. (2003). Processing of low-probability sounds by cortical neurons. Nat. Neurosci. *6*, 391–398.

Vanhatalo, S., Voipio, J., and Kaila, K. (2005). Electroencephalography: Basic Principles, Clinical Applications, and Related Fields, E. Niedermeyer and F. Lopes da Silva, eds. (Philadelphia, PA: Lippincott Williams and Wilkins), pp. 489–493.

Von Stein, A., and Sarnthein, J. (2000). Different frequencies for different scales of cortical integration: from local gamma to long range alpha/theta synchronization. Int. J. Psychophysiol. *38*, 301–313.

Von Stein, A., Chiang, C., and Koenig, P. (2000). Top-down processing mediated by interareal synchronization. Proc. Natl. Acad. Sci. USA *97*, 14748–14753.

Warren, R.M. (1999). Auditory Perception: A new Analysis and Synthesis (Cambridge, UK: Cambridge University Press).

Warren, R.M., Obusek, C.J., and Ackroff, J.M. (1972). Auditory induction: Perceptual synthesis of absent sounds. Science *176*, 1149–1151.

Warren, R.M., Bashford, J.A., Healy, E.W., and Brubaker, B.S. (1994). Auditory induction: Reciprocal changes in alternating sounds. Percept. Psychophys. *55*, 313–322.

Wrightson, J.M., and Warren, R.M. (1981). Incomplete auditory induction of tones alternated with noise: Effects occurring below the pulsation threshold. J. Acoust. Soc. Am. *69*, S105–S106.

Yordanova, J., and Kolev, V. (1998). Single-sweep analysis of the theta frequency band during an auditory oddball task. Psychophysiology *35*, 116–126.

Zatorre, R.J., Belin, P., and Penhune, V.B. (2002). Structure and function of auditory cortex: Music and speech. Trends Cogn. Sci. *6*, 37–46.